Journal of Chromatography, 320 (1985) 23–32
Elsevier Science Publishers B.V., Amsterdam — Printed in The Netherlands

CHROM. 17,327

COMPUTER AIDED ANALYSIS OF ELECTRIC FIELD GRADIENTS WITHIN ISOTACHOPHORETIC BOUNDARIES BETWEEN WEAK ELECTROLYTES

R. A. MOSHER*, W. THORMANN* and M. BIER
Biophysics Technology Laboratory, University of Arizona, Tucson, AZ 85721 (U.S.A.)

SUMMARY

Computer simulations are used to describe the temporal evolution of concentration and potential profiles in isotachophoresis. In contrast to other theoretical treatments of moving boundaries between weak electrolytes, diffusional effects are considered, which allows an exact prediction of boundary shape. The computer predicted shapes of three different electric field gradients between migrating protolytes are analyzed: (i) the commonly observed sigmoidal field increase from the leading to the terminating zone; (ii) the mirror image of such a gradient in the enforced migrational mode; (iii) the steady state "bump" gradient which can be established between a weak acid and its salt. The value of these predictions to the experimentalist is discussed.

INTRODUCTION

Isotachophoresis (ITP) is an electrophoretic separation technique characterized by a set of steady state boundaries, all moving with equal velocity, which represent interfaces between adjacent sample zones[1–3]. Each boundary area contains concentration, conductivity and temperature gradients between two homogeneous zones of different electrolytes. An exact description of such gradients in systems comprised of weak electrolytes can be obtained only by computer modeling[4,5].

A knowledge of the shape of electric field gradients across boundaries has grown steadily in importance in recent years because ITP is in the process of becoming a widely used, high resolution methodology in instrumental analysis[3]. Commercial as well as research instruments are equipped with potential gradient (or conductivity) detectors consisting of sensing microelectrodes. The magnitude of the potential gradient signal along the sample zone can be compared with that of standard substances for identification purposes. Quantitation is accomplished by zone length measurements, *i.e.* the determination of the distances between adjacent electric field gradients. It is the effective or net mobility of the sample which determines detector

* Present address: Division of Chemical and Physical Sciences, Deakin University, Victoria 3217, Australia.

0021-9673/85/$03.30

response. This quantity is given by the product between mobility coefficient and dissociation coefficient[1–3,6–9]. It is therefore strongly influenced by chemical equilibria. The order of zones in an isotachopherogram is an additional qualitative parameter. Usually zones arrange themselves in order of net mobilities which results in a stepwise increase of the electric field from the leading to the terminating electrolyte. However, under certain conditions, this sequence can be inverted thus producing an electric field decrease opposite to the migration direction[2,7–9].

A precise description of ITP boundaries is of critical importance to the analytical applications of the technique. Early attempts to predict the shape of electric field gradients across steady state moving boundaries were restricted to simplified systems comprised of three monovalent strong electrolytes. Longsworth[10] calculated concentration profiles for these systems assuming that the mobilities of the leading and counter constituents were equal and twice as large as the mobility of the displacing component. Approximate numerical solutions without mobility restrictions have been calculated by Coxon and Binder[11]. The electric field gradients have a sigmoidal shape which increases from the leading to the displacing zone. With weak electrolytes this situation may be modified by the presence of superimposed chemical reactions (protolysis, complex equilibria) which contributes to the self-sharpening effect necessary to produce a steady state.

We have used a general mathematical model which predicts the salient features of all the classically recognized methods in electrophoresis, including ITP, to investigate these gradients[4,5]. The model is based upon equations describing conservation of mass and charge, electroneutrality and the component's chemical equilibria. The net mass transport of each component due to electromigration and diffusion is computed. It should be emphasized that this computer implemented model does not require any simplifications concerning the nature of the components in solution. In particular, chemical equilibrium processes as well as the dissociative behavior of the solvent are included. This is in contrast to computer models reported by Ryser[12], Moore[13] and Vaćik and Fidler[14] where only strong electrolytes in indifferent solvents are considered. Radi[15] developed a computer model for ITP systems comprised of strong and/or weak electrolytes. His description of the behavior of weakly ionizing components utilizes the kinetic constants for the association and dissociation reactions of a chemical equilibrium. Such a system is difficult to treat numerically because the rate of proton transfer reactions is *ca.* 10 orders of magnitude greater than that of electrophoretic phenomena. To simplify his calculations Radi specified much lower reaction rates, which allowed him to demonstrate the influence of these reaction velocities on the boundary shape. However, the computed profiles are much broader than those expected. In contrast to this method our program utilizes dissociation constants, which allow a precise prediction of the boundary structure.

In this paper computer simulations which display the evolution of moving and stationary boundaries in ITP systems of weak electrolytes are presented. Three different electric field gradients produced across ITP boundaries between protolytes will be analyzed: (i) the sigmoidal field increase from the leading to the terminating zone which is commonly observed between strong electrolytes; (ii) the mirror image of such a gradient, which is obtained in the presence of an appropriate chemical potential gradient, despite the displacing constituent having the higher net mobility; (iii) the steady state "bump" gradient, established, for example, between a salt of a weak

acid and the acid itself. The value of the computer predictions to the experimentalist is discussed. Laboratory data showing the electric field gradients across various boundaries are given to illustrate the consistency between experiment and computer prediction.

COMPUTER SIMULATION

Our computer model is one-dimensional and assumes the absence of convective flows or thermal gradients. No *ad hoc* stipulations are made concerning pH or voltage gradients, rather these profiles are computed as a part of the solution. The electrophoresis column is overlaid with a set of grid points for discretization of the spatial derivatives. Central differences are used wherever possible, with forward and backward differences used at the boundaries. The resulting ordinary differential equations with time as the independent variable are integrated using software developed on the basis of DARE-P language[16,17].

The inputs required to perform a simulation include the dissociation constants of the compounds, the mobility coefficients of the positive, negative and neutral species, the initial concentration distribution of the compounds in the column, the cross-sectional area and length of the column and the current. The amount of electrophoresis time is also specified. The values used for all presented examples are summarized in Table I. In addition, the simulation of ITP requires enforcement of constant buffer concentrations at the column boundaries. Reactions which occur at the driving electrodes are not allowed to interfere with the components under observation[4]. The outputs from a simulation are the concentrations of each component at each grid point across the column, and the pH and conductivity profiles. The maximum relative local truncation error for these simulations, as computed by the order difference method, is $1.0 \cdot 10^{-4}$.

TABLE I

INPUT DATA FOR COMPUTER SIMULATIONS*

Figure	*Component*	pK_a	*Mobility*** × 10⁴ (cm²/Vsec)*	*Initial conc. (mM) anolyte/catholyte*	*Current density (mA/cm²)*
1	Chloroacetic acid	2.85	4.12	2.0/0	0.6
	Glycolic acid	3.85	4.12	0/3.0	
2	Formic acid	3.75	5.64	10.0/10.0	1.2
	Na^+	–	5.19	0/10.0	
3	Citric acid	3.14	5.64	10.0/10.0	1.2
	Na^+	–	5.19	0/10.0	
4	Papaverine	6.40	1.65	0/2.0	0.4
	Aniline	4.78	3.00	3.0/0	
	Acetic acid	4.76	4.24	3.0/2.0	

* The mesh used for all simulations was 50 segments/cm.

** It was assumed that all species of a component have equal mobilities and that the transport properties are constant throughout the column. The mobility of H_3O^+ was $36.27 \cdot 10^{-4}$ and that of OH^- $19.87 \cdot 10^{-4}$ cm²/Vsec.

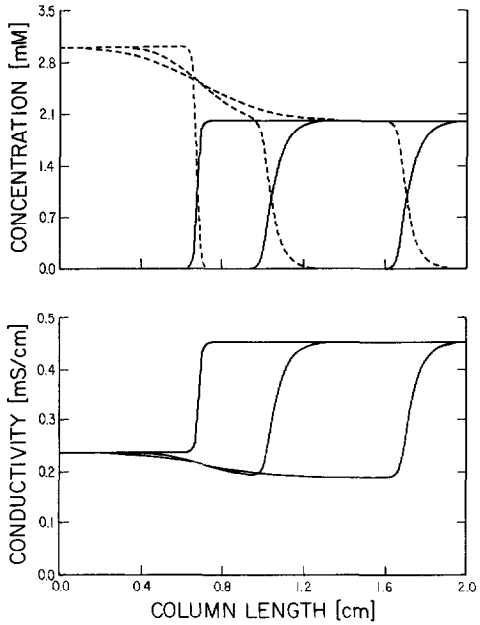

Fig. 1. Upper panel: the computer simulated evolution of a moving boundary formed between chloroacetic acid, the leading component (solid lines) and glycolic acid, the displacing component (dashed lines). The anode is to the right. The profiles are plotted after 0, 20 and 55 min of current (0.6 mA/cm^2) flow. Lower panel: corresponding conductivity profiles. See Tables I and II for additional data.

An example of the computer-predicted evolution of an ITP system of two weak acids is presented in Fig. 1. The solution for each time point was computed at 101 equally spaced grid points over the 2-cm column length. The boundary at zero time occupies seven of the grid points and its shape is calculated by solving the linear diffusion equation with a step as the input. A 2 m*M* solution of chloroacetic acid occupies the anodic end of the column whereas a 3 m*M* solution of glycolic acid was chosen as catholyte. Concentration profiles corresponding to 0, 20, and 55 min of current flow are depicted in Fig. 1. This figure shows the concentration adjustment of the trailing electrolyte as it moves into that part of the column originally occupied by the leading electrolyte. This is completely analogous to the adjustment predicted by Kohlrausch[18] for strong electrolytes. The mobility coefficients of all species of the two acids are assumed to be equal. It follows from this assumption that the concentration of the displacing electrolyte behind the moving boundary is the same as that of the leading electrolyte. It should be emphasized that this mobility restriction is not required by our model. The migrating boundary has reached its steady state shape after *ca.* 10 min. This figure also shows the stationary boundary formed at the initial interface. This dilution boundary never reaches a steady state but continues to diffuse throughout the simulation. The conductivity profiles for the three time points are also presented. This is a system with a sigmoidal increase of the electric field and the pH gradient from the leading to the terminating electrolyte. Additional computer simulated data are presented in Table II.

Fig. 2 presents the computer simulated evolution of a cationic ITP boundary

TABLE II

OUTPUT DATA FROM COMPUTER SIMULATIONS

Figure	*Leading* component*	*Terminating* component*	*Counter component*	*pH leader/ terminator*	*Conductivity leader/terminator (mS/cm)*	*Boundary character*
1	Chloroacetic acid (2.00)	Glycolic acid (2.00)	H_3O^+	2.95/3.33	0.4511/0.1881	Steady state, anionic
2	Na^+ (10.00)	Formic acid (18.06)	$Formate^-$	7.87/2.76	1.0831/0.7147	Steady state, cationic
3	Na^+ (10.00)	Citric acid (18.03)**	$Citrate^-$	7.58/2.48**	1.0831/1.3675**	Non-steady state cationic
4	Papaverine (2.00)	Aniline (2.79)	$Acetate^{-}$***	5.58/4.72	0.1033/0.1154	Enforced, near-steady state, cationic

* The values in brackets represent concentrations in m*M*.
** Steady state value not fully established after 60 min of current flow.
*** The acetate concentration across the boundary increases from 2.00 to 3.15 m*M*.

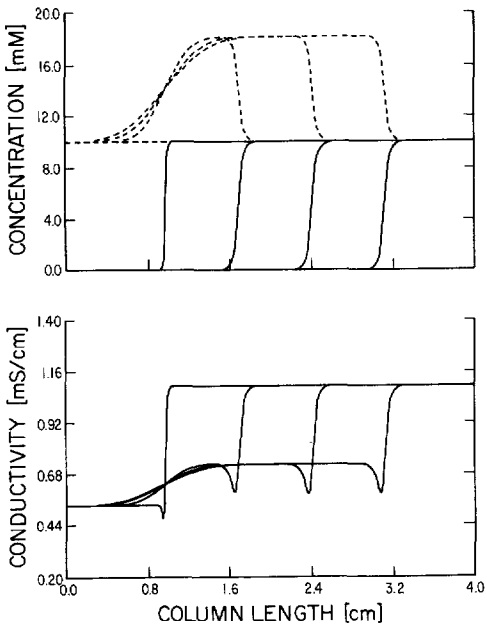

Fig. 2. Upper panel: computer simulated evolution of a boundary between 10 m*M* sodium formate, the leading electrolyte, and formic acid, the displacing electrolyte. The cathode is to the right. The solid lines present the sodium concentrations after 0, 20, 40 and 60 min of current (1.2 mA/cm^2) flow. The dashed lines present the total formate concentration (neutral and charged species). Lower panel: corresponding conductivity profiles. See Tables I and II for additional data.

with 10 m*M* sodium formate as leading electrolyte and formic acid as terminator. Sodium represents the leading and H_3O^+ the terminating constituent. Formate is the common counter component. The solution for each time point was computed at 201 equally spaced points over the 4-cm column length. This example documents the formation of a steady state boundary which migrates towards the cathode. The corresponding conductivity profiles for the four time points are also presented. Concentration, pH and conductivity data outside of the boundary area are listed in Table II. For the examples given in Figs. 1 and 2 the model predicts lower electric fields in the leading zones compared with those in the terminating electrolytes. This is in agreement with the predictions of models based on migration only[19,20]. The sigmoidal shape of the conductivity profile in Fig. 1 also corresponds with predictions made by these simplified models. This is not the case in Fig. 2 however. The electric field gradient between formic acid and sodium formate (at this concentration[20]) is composed of a sigmoidal part on the front side with an additional "bump" on the rear side. This "bump" has a steady state shape. The overall field increase opposite to the migration direction is due to the higher net mobilities of the leading components.

If the net mobility of the leading component in the displacing zone is smaller than that of the terminating component, non-steady state boundaries are produced. Such gradients progressively broaden and are characterized by a field decrease opposite to the migration direction. They are not suitable for ITP analyses. Fig. 3

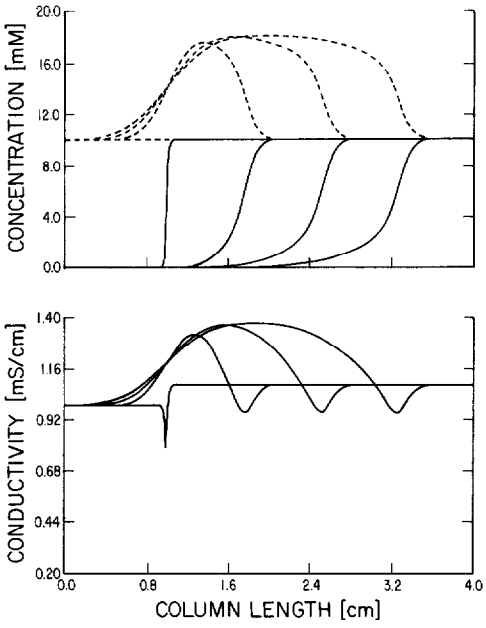

Fig. 3. Upper panel: computer simulated evolution of a non-steady state boundary between 10 m*M* sodium citrate, the leading electrolyte and citric acid, the displacing electrolyte. The cathode is to the right. The solid lines indicate the sodium concentration after 0, 20, 40 and 60 min of current (1.2 mA/cm^2) flow. The dashed lines indicate the total citrate concentration (neutral and charged species). Lower panel: corresponding conductivity profiles. See Tables I and II for additional data.

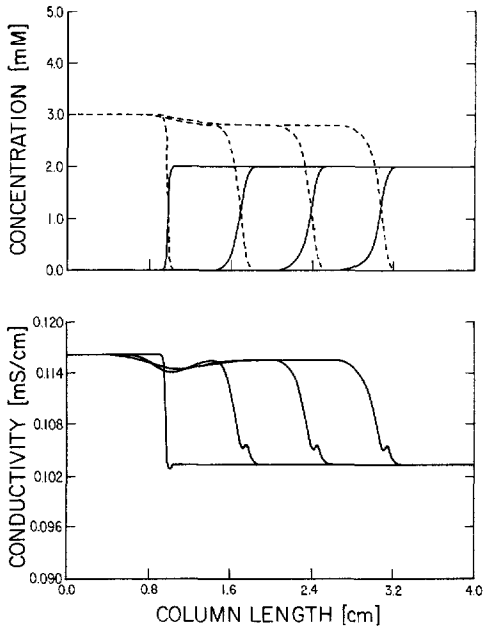

Fig. 4. Upper panel: computer simulated evolution of a boundary between papaverine, the leading component (solid lines), and aniline, the trailing component (dashed lines). Acetate is the counter component. The cathode is to the right. Profiles are presented after 0, 20, 40 and 60 min of current (0.4 mA/cm^2) flow. Lower panel: corresponding conductivity profiles. See Tables I and II for additional data.

displays computer simulated concentration and conductivity profiles between 10 mM sodium citrate and citric acid. The moving boundary clearly broadens as it migrates. This system is very similar to the sodium formate/formic acid of Fig. 2. The only exception is that the pK_a value of citric acid is 0.61 pK units smaller than that of formic acid. The conditions of both simulations were chosen to be consistent with the experimental results of Boček *et al.*[19] and Thormann *et al.*[20]. It should be noted that not all sodium citrate–citric acid systems produce unstable boundaries. It has been shown for such systems[19] that there is a limiting concentration of the leading cation which must be exceeded for a steady state boundary to be produced. The value is 16.8 mM for this case.

The system depicted in Fig. 4 uses a mixture of papaverine (leading component) and acetic acid (counter component) as leading electrolyte and aniline and acetic acid as terminating electrolyte. A boundary migrating towards the cathode is produced across which the conductivity increases from the leading to the terminating electrolyte. It, however, is not quite a steady state boundary. This can be most easily seen by inspecting the trailing edge of the papaverine profile, which broadens very slowly. This slight expansion continued for an additional 180 min of simulated electrophoresis, thus it appears not to be merely a case of a slow approach to the steady state. Although not a steady state boundary, it is sufficiently stable to be useful experimentally[7]. The nearly steady state nature of this boundary in the presence of a conductivity decrease across the boundary in the direction of migration is due to the pH gradient which is also present. The higher pH in the leading zone (see Table

II), compared with the terminator, has a stabilizing influence on the boundary. The aniline which crosses the boundary becomes deprotonated, thus reducing its net mobility. The papaverine which crosses the boundary experiences an increase in net mobility due to protonation. This phenomenon was experimentally observed by Gebauer and Boček and discussed with their zone existence diagram[7]. Additional examples of other cationic boundaries have also been reported by these authors[8]. Anionic enforced migration was observed by Mikkers *et al.*[9] and Everaerts *et al.*[2]. Such systems are also stabilized by the presence of a pH gradient from leader to terminator. This simulation is the first precise description of the boundary structure in the enforced migration mode in ITP, where zones do not occur in order of decreasing net mobilities. It is interesting to note that the electric field across the papaverine/aniline boundary has a small shoulder on its front side. However, the pH gradient (not displayed) is sigmoidal.

RESULTS AND DISCUSSION

The electric field gradients between ITP zones generally produce steplike responses from potential gradient detectors. Superimposed "bumps" are often considered to be artifacts, resulting from processes such as adsorption/desorption on the microsensing electrodes. While in some cases this might be true, the computer simulations presented in this paper predict that steady state "bump" gradients can be produced by the electrophoretic system as well (Fig. 2). Such boundary shapes are definitely measurable (refs. 8, 19 and 20; Fig. 5). The experiments presented in Fig. 5 were carried out in an ITP column of rectangular cross-section[21]. This apparatus is equipped with an array of 255 potential gradient sensors. The boundaries were monitored as they moved across one sensor. Detector response was recorded by a strip chart recorder. Pherogram "a" was taken under constant current. The "bump"

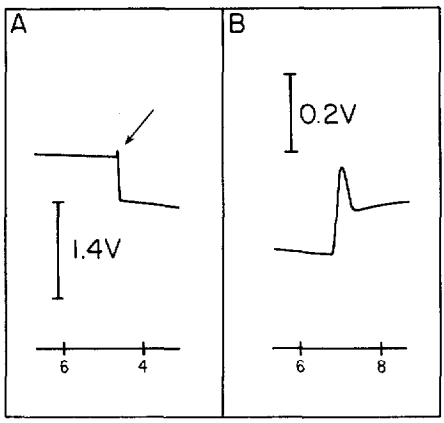

Fig. 5. Experimental electric field gradients across a moving boundary between the leading electrolyte of 10 m*M* sodium formate and formic acid as the displacing component. A capillary (cross section about 0.004 cm^2) type apparatus with potential gradient sensors was used. Pherogram "a" was monitored under a constant current of 100 μA. The x-axis scale is the time in minutes after current application. The arrow indicates the detected electric field "bump". Pherogram "b" was detected under constant voltage conditions. The current at the time of detection was *ca.* 14 μA.

TABLE III

MOBILITY* REQUIREMENTS AND MIGRATION MODES

$M_L^v > M_L^\lambda > M_V^v$	Steady-state migration (electric field increase)
$M_L^v > M_V^v > M_L^\lambda$	Enforced migration (electric field decrease)
$M_L^v < M_V^v$	Non-steady state migration (electric field decrease)

* The net mobility of a component j in the leading zone λ and the displacing zone v are denoted by M_j^λ and M_j^v respectively. L refers to the leading component and V refers to the terminating constituent.

is very sharp and therefore not fully detected because of the signal dampening of the recorder. Reducing the current density permits the monitoring of the actual shape as shown in pherogram "b". This experiment was taken with an applied constant voltage rather than constant current.

Most of the theoretical treatments of electrophoretic processes in the literature neglect diffusion for purposes of simplification and are based on migration only. These theories can describe the composition of the areas outside of ITP boundaries but not the shape of a boundary. They can also predict the fundamental criteria which have to be fulfilled for the formation of an electric field increase across the boundary opposite to the displacement direction. In general this necessitates a higher net mobility for the leading component than for the terminator, but this is not the sole requirement[22]. When all components are present in both electrolytes of a discontinuous buffer system, the concentration ratio of the leading to the terminating component must be lower in the electrolyte behind the moving boundary than it is in the leading zone. The models based on migration only are also capable of predicting the velocity of a steady state moving boundary. These results are in good agreement with our computer model[5].

Self-sharpening effects are necessary for the establishment of steady state boundaries. The simulation results which have been presented illustrate the factors which produce such effects. Generally, the self-sharpening mechanism is characterized by the balance between diffusional spreading and migrational sharpening due to the field strength variation across the boundary. Chemical equilibria further influence the boundary width[5]. A chemical potential gradient may even stabilize a system which is lacking the appropriate potential gradient. This is the case with the papaverine–aniline system. In such a system, diffusional and migrational spreading are nearly balanced by the sharpening effect of protolysis. A rapidly broadening boundary would be established in the absence of this constraint as is shown with the sodium citrate–citric acid boundary. Table III summarizes the mobility relationships between the leading and terminating components which are required for the establishment of the various migration modes.

CONCLUSIONS

Computer modeling is a valuable aid to the understanding of electrophoretic processes. It constitutes the only methodology at hand for describing concentration and conductivity profiles as functions of time and location. The model enabled us to explore the nature of the potential gradient across several different types of boundaries; sigmoidal, "bump" and mirror image gradients. A knowledge of these gradients

provides an understanding of the self-sharpening effects which produce a steady state. The boundaries discussed involve proton transfer reactions which, if properly applied, sharpen the boundary. Thus, both the chemical and the electric field gradients can act against diffusion to maintain the steplike concentration distributions across adjacent zones. This occurs in acidic systems when pH and electric field gradients are concomitantly increasing from leading to terminating zones (Fig. 1, refs. 5 and 20). An electric field decrease can be stabilized by strong chemical sharpening. We have referred to this as enforced migration. Many other chemical reactions in addition to proton transfer can be used in this application, especially complex formation[23]. The only general requirement is that the reaction must be fast. The average lifetime of the ionic constituents involved in the formation of the zone boundary must be smaller than the transit time through the boundary thickness under the applied electric field. This calls for half-lives of ligand exchange reactions of less than 1 msec[24]. The computer simulated sodium citrate–citric acid boundary is an example where no steady state is produced. In this case the flow of citrate from the leading zone through the boundary is smaller than that of H^+ in the other direction. This, together with the dispersion due to the electric field variation and diffusion, results in the gradual broadening of the gradient.

ACKNOWLEDGEMENTS

This work was supported in part by NASA grant NSG-7333 and by NSF grant CPE-8311125.

REFERENCES

1 E. Schumacher and T. Studer, *Helv. Chim. Acta*, 47 (1964) 957.
2 F. M. Everaerts, J. L. Beckers and Th. P. E. M. Verheggen, *Isotachophoresis—Theory, Instrumentation and Applications*, Elsevier, Amsterdam, 1976.
3 P. Boček, *Topics Current Chem.*, 95 (1981) 131.
4 M. Bier, O. A. Palusinski, R. A. Mosher and D. A. Saville, *Science*, 219 (1983) 1281.
5 W. Thormann and R. A. Mosher, *Trans. SCS*, 1 (1984) 81.
6 W. Thormann, *Separ. Sci. Technol.*, 19 (1984) 455.
7 P. Gebauer and P. Boček, *J. Chromatogr.*, 267 (1983) 49.
8 P. Gebauer and P. Boček, *J. Chromatogr.*, 242 (1982) 245.
9 F. E. P. Mikkers, F. M. Everaerts and J. A. F. Peek, *J. Chromatogr.*, 168 (1979) 317.
10 L. G. Longsworth, *J. Amer. Chem. Soc.*, 66 (1944) 449.
11 M. Coxon and M. J. Binder, *J. Chromatogr.*, 95 (1974) 133.
12 P. Ryser, *Dissertation*, University of Bern, Bern, 1976.
13 G. T. Moore, *J. Chromatogr.*, 106 (1975) 1.
14 J. Vaćik and V. Fidler, in F. M. Everaerts (Editor), *Analytical Isotachophoresis*, Elsevier, Amsterdam, 1981, p. 19.
15 P. Radi, *Thesis*, University of Bern, Bern, 1982.
16 G. A. Korn and J. V. Wait, *Digital Continuous System Simulation*, Prentice-Hall, Englewood Cliffs, NJ, 1978.
17 A. Graham, O. A. Palusinski, R. A. Mosher, M. Bier and D. A. Saville, *Proceedings of the 10th IMACS World Congress on System Simulation and Scientific Computations*, International Association for Mathematics and Computers in Simulation, Montreal, 1982, Vol. 4, p. 92.
18 F. Kohlrausch, *Ann. Phys. Chem. NF*, 62 (1897) 209.
19 P. Boček, P. Gebauer and M. Deml, *J. Chromatogr.*, 217 (1981) 209.
20 W. Thormann, D. Arn and E. Schumacher, *Electrophoresis*, in press.
21 E. Schumacher, W. Thormann and D. Arn, in F. M. Everaerts (Editor), *Analytical Isotachophoresis*, Elsevier, Amsterdam, 1981, p. 33.
22 R. A. Mosher and W. Thormann, *Electrophoresis*, in press.
23 P. Boček, I. Miedziak, M. Deml and J. Janák, *J. Chromatogr.*, 137 (1977) 83.
24 E. Schumacher, *Helv. Chim. Acta*, 40 (1957) 2322.